

RESEARCH ARTICLE



Analysis of the Optical Properties and Electronic Structure of Semiconductors of the Cu_2NiXS_4 ($X = \text{Si, Ge, Sn}$) Family as New Promising Materials for Optoelectronic Devices

Dilshod Nematov^{1,*} ¹S.U. Umarov Physical-Technical Institute of the National Academy of Sciences of Tajikistan, Tajikistan

Abstract: In this work, the optoelectronic characteristics of kesterites of the Cu_2NiXS_4 system ($X = \text{Si, Ge, Sn}$) were studied. The electronic properties of the Cu_2NiXS_4 ($X = \text{Si, Ge, Sn}$) system were studied using first-principles calculations within the framework of density functional theory. For calculations, *ab initio* codes VASP and Wien2k were used. The high-precision modified Beke-Jones (mBJ) functional and the hybrid HSE06 functional were used to estimate the band gap, electronic, and optical properties. Calculations have shown that when replacing Si with Ge and Sn, the band gap decreases from 2.58 eV to 1.33 eV. Replacing Si with Ge and Sn reduces the overall density of electronic states. In addition, new deep (shallow) states are formed in the band gap of these crystals, which is confirmed by the behavior of their optical properties. The obtained band gap values are compared with existing experimental measurements, demonstrating good agreement between HSE06 calculations and experimental data. The nature of changes in the dielectric constant, absorption capacity, and optical conductivity of these systems depending on the photon energy has also been studied. The statistical dielectric constant and refractive index of these materials were found. The results will help increase the amount of information about the properties of the materials under study and will allow the use of these compounds in a wider range of optoelectronic devices, in particular, in solar cells and other devices that use solar radiation to generate electric current.

Keywords: band gap, kesterites, optical properties, solar cells, absorption coefficient, dielectric constant, photoelectric applications

1. Introduction

One of the factors contributing to global warming is the burning of fossil fuels, which increases the concentration of carbon dioxide in the atmosphere, warming the planet and changing the climate [1–3]. The Earth absorbs a significant portion of the light emitted by the Sun when it reaches its surface. As a result of heating the planet with this energy, its surface emits infrared radiation. The greenhouse effect, which causes global warming, occurs when carbon dioxide in the atmosphere absorbs much of the incoming thermal radiation and reflects it back to the Earth's surface [4, 5]. It is known that electricity generation emits about 40% of greenhouse gases into the atmosphere [6, 7]. However, the world now obtains 80% of its energy from fossil fuels (oil, coal, and gas), which also contribute to environmental pollution and the daily depletion of these natural supplies [8]. Thus, in light of the anticipated need for electricity worldwide and the 21st century green energy agenda, the issue of the development of alternative and renewable energy sources is brought up, and the potential for transforming non-traditional energy into electricity is examined [9].

Alternative sources such as windmills, moisture-to-electricity converters, thermoelectric generators, photovoltaic (PV) converters (solar panels), solar thermophotovoltaic converters, and the use of geothermal waters have a positive effect on the air environment, but they are not available everywhere. One of the effective natural sources of alternative energy is the synthesis and optimization of the properties of new nanomaterials to create solar energy converters into electricity, which is very effective and environmentally friendly compared to many other methods [1–9]. The great growth potential of this alternative energy industry is due to such global factors as the need to ensure national energy security and the rising cost of fossil energy sources. Alternative energy has other unique advantages: for example, solar energy is available to everyone, free, practically inexhaustible, and the process of converting it into electrical energy does not have a negative impact on the environment [10–13].

In recent years, photovoltaics has been rapidly developing for the developed of which, in addition to silicon and perovskites, many types of crystalline materials have been developed and proposed [14–21]. One of these promising and promising materials is kesterite materials with the general formula A_2BCD_4 ($A = \text{Cu, Ag; B = Zn, Cd, Ni, Mg, \dots; C = \text{Sn, Ge, Si; D = S, Se}$) [22]. Since their emergence as so-called “Third generation generators,” PV systems have been hailed as an environmentally and economically viable alternative to conventional technologies for solving the world's

*Corresponding author: Dilshod Nematov, S.U. Umarov Physical-Technical Institute of the National Academy of Sciences of Tajikistan, Tajikistan. Email: dilnem@phti.tj

energy, safety, and environmental problems [23–25]. However, despite the obvious achievements in this area, the development and research of the fundamental properties of potentially new kesterite PV materials are of great importance for improving the performance of devices based on them.

Because of their direct band gap in the 1.0–2.5 eV region, the most extensively used kesterite crystals based on the $\text{Cu}_2\text{ZnSnS}_4$ and $\text{Cu}_2\text{ZnSnSe}_4$ (CZTSSe) system are utilized in the industrial manufacture of solar panels [26]. Kesterite's range of use is increased by the adjustable band gap, which also enables task-specific adjustment for ideal spectral matching [27]. Furthermore, they are excellent candidates for the production of solar energy due to their p-type conductivity and high optical absorption coefficient ($>10^4 \text{ cm}^{-1}$) [28]. Additionally, this allows for the kesterite film to be thinned down to a point where the solar panel's cost can be decreased without sacrificing efficiency [28]. The efficiency of kesterite-based solar cells has recently risen from 12.6% to 13.6% [29–31]. However, the performance of solar cells based on this material is still far from the theoretical limit, indicating that the efficiency potential of kesterite is still little exploited. The reason for the poor performance of CZTSSe is mainly due to their high open circuit voltage deficit, which has been repeatedly reported in research papers [32–35]. This is due to fluctuations in the band gap and potential induced by crystalline disorder between elements A and B sites of kesterite which occurs at the structural and electronic levels [32–35]. Existing problems force researchers to develop new analogues of CZTSSe; however, obtaining new perovskites including some members of the Cu_2NiXS_4 family ($X = \text{Si, Ge, Sn}$) is labor-intensive work due to the complex single-phase growth of kesterite while obtaining a homogeneous and high-quality layer free of secondary phases [34, 35]. Sometimes the final synthesis of kesterite materials results in many undesirable solid solutions, which complicate the work [36], and some resulting materials with a kesterite structure may have undesirable properties. Therefore, in recent years, preliminary prediction of properties applied to the synthesis of materials has become an integral tradition among the solid state community.

In this regard, recently the properties of kesterites have also been studied by various theoretical methods, as a result of which the efficiency of solar cells based on them is constantly increasing [25–36]. Density functional theory (DFT) is a potent theoretical approach that has gained significant traction in the last 10 years as a major tool for the theoretical study of solid materials. Its potent approach accounts for the behavior of electrons in all atomic molecular environments and offers a highly accurate reformulation of quantum mechanical calculations of solids. This is because contemporary computing clusters can solve the Kohn–Sham equations efficiently [37–45]. However, these formulas are predicated on a single estimate, that of the exchange–correlation energy, which accounts for the precision of quantum computations. Here, many of the basic characteristics of compounds based on the Cu_2NiXS_4 ($X = \text{Si, Ge, Sn}$) family still remain poorly studied and correspond to the current topic requiring in-depth research, despite the annual increase in publications devoted to the study of the properties of kesterites.

In this work, using quantum chemical calculations within the framework of DFT, the electronic and optical properties of kesterites of the Cu_2NiXS_4 ($X = \text{Si, Ge, Sn}$) family are studied, a detailed study and disclosure of which is important for the appropriate selection of the synthesized material for specific applications.

2. Materials and Methods

Ab initio quantum chemical calculations within the framework of DFT were carried out on the basis of data on crystal lattices published in Nematov [46], obtained after complete relaxation of lattice parameters using the VASP package [47] and the SCAN functional [48–50]. In this case, electronic and ion relaxation was achieved at a cutoff energy of 550 eV and $3 \times 3 \times 3$ k-points. The band gap, electronic structure, and optical properties of Cu_2NiXS_4 ($X = \text{Si, Ge, Sn}$) systems were studied using the VASP and Wien2k quantum chemical simulation codes using the hybrid functional HSE06 [51] and the modified TB-mBJ functional [52]. The optimal plane wave cutoff value K_{max} was selected as $6.0 \text{ Ry}^{1/2}$. The Kohn–Sham equations were solved using LAPW. Kesterite crystals of the tetragonal system (symmetry group I-4) were chosen as the structures under study. The following valence electrons were considered: Si: $3s^2 3p^2$, Cu: $3d^{10} 4s^1$, Sn: $4d^{10} 5s^2 5p^2$, Ni: $3d^{10} 4s^2$, Ge: $3d^{10} 4s^2 4p^2$, and S: $3s^2 3p^4$.

3. Results and Discussion

The energy band distribution diagram, the band energy's dependence on the density of electronic states (DOS), and the band gap's numerical values are used to evaluate the electronic characteristics of the Cu_2NiXS_4 ($X = \text{Si, Ge, and Sn}$) system. Table 1 compares the band gap values we calculated within DFT – HSE06 with the results of experimental measurements by independent authors.

Table 1
Comparison of the calculated value of the band gap of the $\text{Cu}_2\text{NiSiS}_4$, $\text{Cu}_2\text{NiGeS}_4$, and $\text{Cu}_2\text{NiSnS}_4$ system with literature data

	Band gap, eV		
	This work	Literature	
	HSE06	Calc.	Experimental
$\text{Cu}_2\text{NiSiS}_4$	2.560	–	–
$\text{Cu}_2\text{NiGeS}_4$	1.802	1.13 ^a	1.8 ^a
$\text{Cu}_2\text{NiSnS}_4$	1.321	1.26 ^b	1.31 ^c , 1.38 ^d

^aBeraich et al. [53]

^bChen and Persson [54]

^cDeepika and Meena [55]

^dKamble et al. [56]

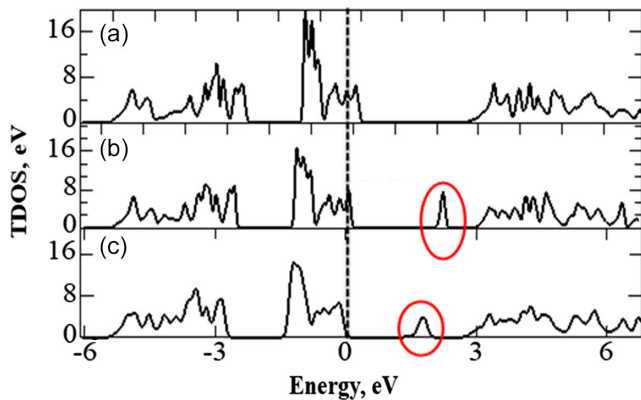
As shown in Table 1, the results of band gap calculations of $\text{Cu}_2\text{NiSnS}_4$, $\text{Cu}_2\text{NiGeS}_4$ crystals obtained from the HSE06 functional are in good agreement with experiment.

The total density of electronic states of $\text{Cu}_2\text{NiSnS}_4$, $\text{Cu}_2\text{NiGeS}_4$, and $\text{Cu}_2\text{NiSiS}_4$ semiconductor crystals was then analyzed using mBJ calculations. The results of calculations of the total density of electronic states for $\text{Cu}_2\text{NiSnS}_4$, $\text{Cu}_2\text{NiGeS}_4$, and $\text{Cu}_2\text{NiSiS}_4$ crystals are shown in Figure 1 (a–c).

The results shown in Figure 2 demonstrate that the band gap lowers and the Fermi levels move toward the valence band when Si is substituted with Ge and Sn. Conversely, it is evident that the density of states drops when Sn takes the place of Si. In this case, new electronic states are formed in the energy gap of $\text{Cu}_2\text{NiGeS}_4$ and $\text{Cu}_2\text{NiSnS}_4$, which are important from the point of view of using the material in electronic devices.

To justify the change in the band gap width, it is necessary to analyze the spectra of the optical properties of the materials under study. Calculated optical properties of materials, including their

Figure 1
Total density of electronic states for $\text{Cu}_2\text{NiSiS}_4$ (a), $\text{Cu}_2\text{NiGeS}_4$ (b), and $\text{Cu}_2\text{NiSnS}_4$ (c)



absorption coefficient and refractive index, provide information about what type of response these materials will exhibit when photons are incident on them [57]. The optical properties of the Cu_2NiXS_4 ($X = \text{Si, Ge, Sn}$) system were investigated based on the calculation of their real (ϵ_1) and imaginary (ϵ_2) parts of the dielectric functions. The real part shows the energy-saving capacity of a material, which is something that is assumed to be inherent in all materials at zero energy or zero frequency limit. Figure 2 (a) and (b) shows the curves of ϵ_1 and ϵ_2 versus the energy of incident photons for kesterites of the Cu_2NiXS_4 ($X = \text{Si, Ge, Sn}$) family.

From Figure 2(a), it can be seen that at the highest photon energies, all these materials, namely kesterite containing silicon, exhibit metallic behavior. That is, a negative value of the real part indicates the possession of a metallic nature at high energies. This makes it possible to estimate the metallicity fractions of materials using a real function, which shows feedback from the optical band gap. For solar devices, the

behavior of these materials indicates the energy gain, whereas the imaginary component of the dielectric function indicates the compound's absorptive capacity. This provides information about how the material reacts when exposed to electromagnetic radiation [58–61]. According to Figure 2(b), the replacement of Si with Ge and Sn leads to an increase in the absorption coefficient of the materials under study in the IR and visible radiation range, which is important for the use of materials in solar panels.

The results displayed in Figure 3 make it evident that adding germanium and tin in place of silicon raises the Cu_2NiXS_4 ($X = \text{Si, Ge, Sn}$) system's refractive index (n). In some energy ranges, the refractive index falls drastically below unity after reaching its maximum value. Furthermore, we can deduce from the expression $n = c/v$ that a refractive index value less than one means that the incident radiation's phase velocity is greater than c , which allows the incident rays to pass through the material and turn it transparent to incoming radiation [62, 63]. Table 2 shows the static values of $\epsilon_{1x}(0)$, $\epsilon_{2z}(0)$, and n according to the DFT-mBJ-WIEN2k calculations.

Beyond the Fermi level, it is known that photon absorption excites occupied states toward unoccupied states. It is known as "optical conduction" when the photons cross the interband transition and as "interband absorption" when they are absorbed. When light is subjected to an electric field, conductivity is known as optical conductivity. Figures 4 and 5 display the computed spectra of the real and imaginary components of the optical conductivity of the systems that are being studied. It is also evident from these spectra that adding Ge and Sn to Si results in improved photoconductivity.

Judging by Figures 4 and 5, optical conductivity for the $\text{Cu}_2\text{NiGeS}_4$ and $\text{Cu}_2\text{NiSnS}_4$ system begins at energies lower than in the case of $\text{Cu}_2\text{NiSiS}_4$. From the data shown in Figure 5, it is clear that these materials actively absorb light even at low photon energies, namely $\text{Cu}_2\text{NiSnS}_4$ is sensitive even to rays with an energy of 0.7 eV. $\text{Cu}_2\text{NiSiS}_4$ also begins to be activated in the energy range above 1.3 eV, having the highest photoconductivity when absorbing short-wavelength radiation [64–70].

Figure 2
Real (a) and imaginary part (b) dielectric constant of kesterites of the Cu_2NiXS_4 ($X = \text{Si, Ge, Sn}$) family

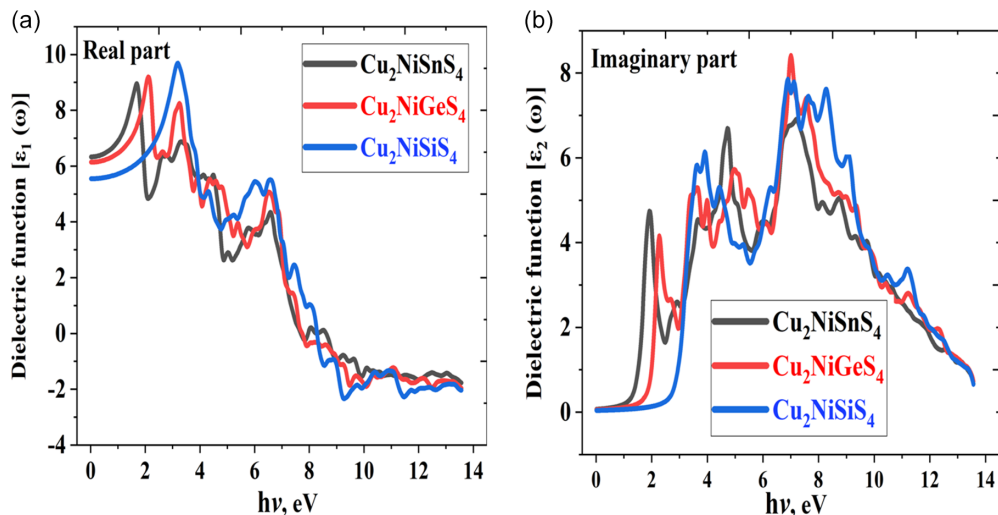


Figure 3
Calculated refractive index spectra of the Cu_2NiXS_4 (X = Si, Ge, Sn) system as a function of photon energy

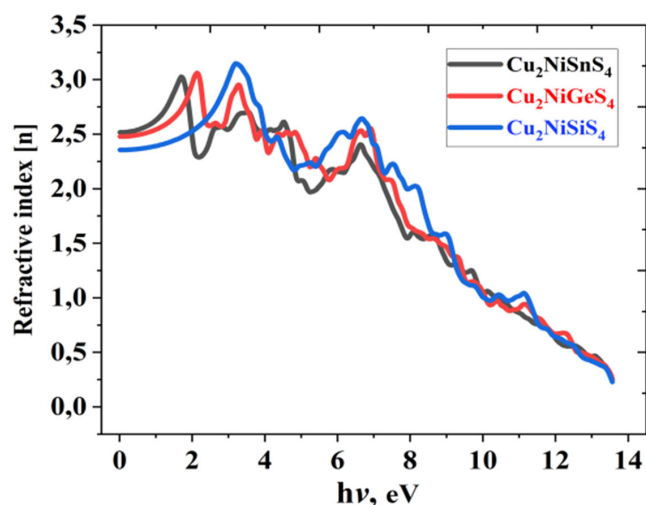


Figure 4
Photon energy-dependent spectra of the real part of the optical conductivity of the Cu_2NiXS_4 (X = Si, Ge, Sn) system

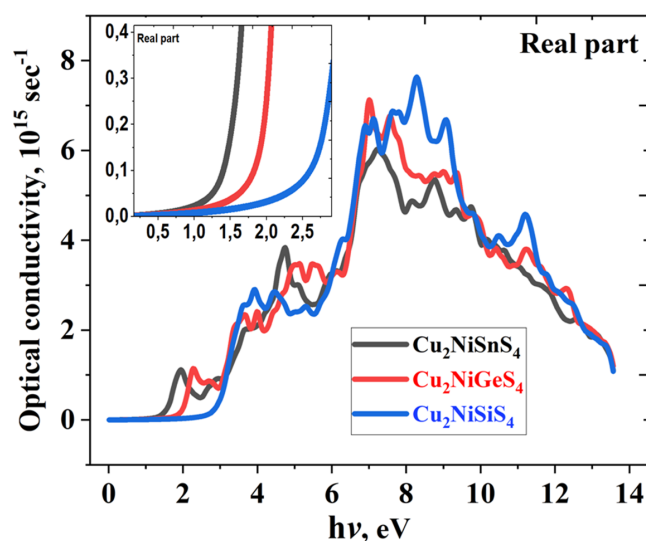
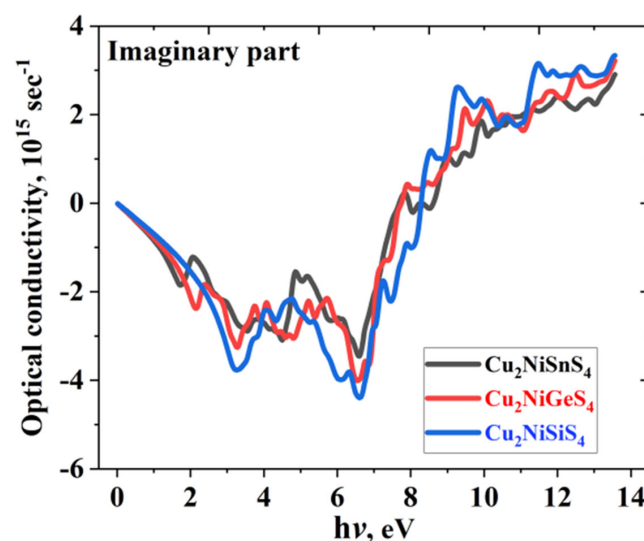


Table 2

Calculated values of statistical dielectric constant and refractive index for kesterites of the Cu_2NiXS_4 (X = Si, Ge, Sn) family

System	$\epsilon_1^x(0)$	$\epsilon_2^z(0)$	n
$\text{Cu}_2\text{NiSiS}_4$	5.68	5.61	2.52
$\text{Cu}_2\text{NiGeS}_4$	6.11	6.46	2.48
$\text{Cu}_2\text{NiXSnS}_4$	6.46	6.88	2.36

Figure 5
Energy-dependent spectra of the imaginary part of the optical conductivity of photons of the Cu_2NiXS_4 (X = Si, Ge, Sn) system



4. Conclusion

The mBJ exchange correlation potential is employed in this study to simulate the electrical and optical characteristics of Cu_2NiXS_4 (X = Si, Ge, Sn). Even though the Cu_2NiXS_4 (X = Si, Ge, and Sn) system's members differ in composition and structure, the permittivity curves and primary optical spectra of all of them exhibit very comparable properties in the infrared and visible radiation ranges. The optical absorption coefficient ($>10^4 \text{ cm}^{-1}$) in the infrared and visible light energy ranges has been discovered to be relatively substantial, and it is proportional to the imaginary part of the permittivity.

Funding Support

The work was supported financially by the International Foundation for Humanitarian Cooperation of the CIS within the framework of a scientific project at the expense of a grant from the International Innovation Center for Nanotechnologies of the CIS (GRANT No. 23-112).

Ethical Statement

This study does not contain any studies with human or animal subjects performed by the author.

Conflicts of Interest

The author declares that he has no conflicts of interest to this work.

Data Availability Statement

Data sharing is not applicable to this article as no new data were created or analyzed in this study.

References

- [1] Jones, M. W., Peters, G. P., Gasser, T., Andrew, R. M., Schwingshackl, C., Gütschow, J., . . . , & Le Quéré, C. (2023). National contributions to climate change due to historical emissions of carbon dioxide, methane, and nitrous oxide since 1850. *Scientific Data*, 10(1), 155. <https://doi.org/10.1038/s41597-023-02041-1>
- [2] Voumik, L. C., Ridwan, M., Rahman, M. H., & Raihan, A. (2023). An investigation into the primary causes of carbon dioxide releases in Kenya: Does renewable energy matter to reduce carbon emission? *Renewable Energy Focus*, 47, 100491. <https://doi.org/10.1016/j.ref.2023.100491>
- [3] Whiteside, M., & Herndon, J. M. (2023). Humic like substances (HULIS): Contribution to global warming and stratospheric ozone depletion. *European Journal of Applied Sciences*, 11(2), 325–346. <https://doi.org/10.14738/aivp.112.14363>
- [4] Aakko-Saksa, P. T., Lehtoranta, K., Kuittinen, N., Järvinen, A., Jalkanen, J. P., Johnson, K., . . . , & Timonen, H. (2023). Reduction in greenhouse gas and other emissions from ship engines: Current trends and future options. *Progress in Energy and Combustion Science*, 94, 101055. <https://doi.org/10.1016/j.pecs.2022.101055>
- [5] Weart, S. R. (2023). Are there simple models of global warming? *The Physics Teacher*, 61(6), 516–518. <https://doi.org/10.1119/5.0128940>
- [6] Andrews, S. S. (2023). *Light and waves: A conceptual exploration of Physics*. Germany: Springer. <https://doi.org/10.1007/978-3-031-24097-3>
- [7] Voumik, L. C., Islam, M. A., Ray, S., Mohamed Yusop, N. Y., & Ridzuan, A. R. (2023). CO₂ emissions from renewable and non-renewable electricity generation sources in the G7 countries: Static and dynamic panel assessment. *Energies*, 16(3), 1044. <https://doi.org/10.3390/en16031044>
- [8] Sinclair, U. (2020). This fossil fuel project is essential. In M. Jaccard (Ed.), *The citizen's guide to climate success: Overcoming myths that hinder progress* (pp. 76–94). Cambridge University Press. <https://doi.org/10.1017/9781108783453>
- [9] Kumar, A., & Prajapati, S. (2023). *Solar powered wastewater recycling*. USA: CRC Press. <https://doi.org/10.1201/9781003407690>
- [10] Fraser, T., Chapman, A. J., & Shigetomi, Y. (2023). Leapfrogging or lagging? Drivers of social equity from renewable energy transitions globally. *Energy Research & Social Science*, 98, 103006. <https://doi.org/10.1016/j.erss.2023.103006>
- [11] Sayed, E. T., Olabi, A. G., Elsaid, K., Radi, M. A., Alqadi, R., & Abdelkareem, M. A. (2023). Recent progress in renewable energy based-desalination in the Middle East and North Africa MENA region. *Journal of Advanced Research*, 48, 125–156. <https://doi.org/10.1016/j.jare.2022.08.016>
- [12] Yang, Y., Bremner, S., Menictas, C., & Kay, M. (2022). Modelling and optimal energy management for battery energy storage systems in renewable energy systems: A review. *Renewable and Sustainable Energy Reviews*, 167, 112671. <https://doi.org/10.1016/j.rser.2022.112671>
- [13] Zhang, Y., Anoopkumar, A. N., Aneesh, E. M., Pugazhendhi, A., Binod, P., Kuddus, M., . . . , & Sindhu, R. (2023). Advancements in the energy-efficient brine mining technologies as a new frontier for renewable energy. *Fuel*, 335, 127072. <https://doi.org/10.1016/j.fuel.2022.127072>
- [14] Almora, O., Baran, D., Bazan, G. C., Cabrera, C. I., Erten-Ela, S., Forberich, K., . . . , & Brabec, C. J. (2023). Device performance of emerging photovoltaic materials (Version 3). *Advanced Energy Materials*, 13(1), 2203313. <https://doi.org/10.1002/aeam.202203313>
- [15] Bellucci, A., Linares, P. G., Villa, J., Martí, A., Datas, A., & Trucchi, D. M. (2022). Hybrid thermionic-photovoltaic converter with an In_{0.53}Ga_{0.47}As anode. *Solar Energy Materials and Solar Cells*, 238, 111588. <https://doi.org/10.1016/j.solmat.2022.111588>
- [16] Dada, M., Popoola, P., Alao, A., Olalere, F., Mtileni, E., Lindokuhle, N., & Shamaine, M. (2023). Functional materials for solar thermophotovoltaic devices in energy conversion applications: A review. *Frontiers in Energy Research*, 11, 1124288. <https://doi.org/10.3389/fenrg.2023.1124288>
- [17] Huang, Y. T., Kavanagh, S. R., Scanlon, D. O., Walsh, A., & Hoye, R. L. Z. (2021). Perovskite-inspired materials for photovoltaics and beyond—From design to devices. *Nanotechnology*, 32(13), 132004. <https://doi.org/10.1088/1361-6528/abc6fd>
- [18] Josephine, E. N., Ikponmwosa, O. S., & Ikhioya, I. L. (2023). Synthesis of SnS/SnO nanostructure material for photovoltaic application. *East European Journal of Physics*, (1), 154–161. <https://doi.org/10.26565/2312-4334-2023-1-19>
- [19] Luceño-Sánchez, J. A., Díez-Pascual, A. M., & Peña Capilla, R. (2019). Materials for photovoltaics: State of art and recent developments. *International Journal of Molecular Sciences*, 20(4), 976. <https://doi.org/10.3390/ijms20040976>
- [20] Rafin, S. M. S. H., Ahmed, R., & Mohammed, O. A. (2023). Wide band gap semiconductor devices for power electronic converters. In *Fourth International Symposium on 3D Power Electronics Integration and Manufacturing*, 1–8. <https://doi.org/10.1109/3d-peim55914.2023.10052586>
- [21] Yao, H., Wang, J., Xu, Y., Zhang, S., & Hou, J. (2020). Recent progress in chlorinated organic photovoltaic materials. *Accounts of Chemical Research*, 53(4), 822–832. <https://doi.org/10.1021/acs.accounts.0c00009>
- [22] Chen, S., Yang, J. H., Gong, X. G., Walsh, A., & Wei, S. H. (2010). Intrinsic point defects and complexes in the quaternary kesterite semiconductor Cu₂ZnSnS₄. *Physical Review B*, 81(24), 245204. <https://doi.org/10.1103/physrevb.81.245204>
- [23] Chen, S., Gong, X. G., Walsh, A., & Wei, S. H. (2010). Defect physics of the kesterite thin-film solar cell absorber Cu₂ZnSnS₄. *Applied Physics Letters*, 96(2), 021902. <https://doi.org/10.1063/1.3275796>
- [24] Steinhagen, C., Panthani, M. G., Akhavan, V., Goodfellow, B., Koo, B., & Korgel, B. A. (2009). Synthesis of Cu₂ZnSnS₄ nanocrystals for use in low-cost photovoltaics. *Journal of the American Chemical Society*, 131(35), 12554–12555. <https://doi.org/10.1021/ja905922j>
- [25] Wang, H. (2011). Progress in thin film solar cells based on Cu₂ZnSnS₄. *International Journal of Photoenergy*, 2011, 801292. <https://doi.org/10.1155/2011/801292>
- [26] Persson, C. (2010). Electronic and optical properties of Cu₂ZnSnS₄ and Cu₂ZnSnSe₄. *Journal of Applied Physics*, 107(5), 053710. <https://doi.org/10.1063/1.3318468>
- [27] Haight, R., Haensch, W., & Friedman, D. (2016). Solar-powering the Internet of Things. *Science*, 353(6295), 124–125. <https://doi.org/10.1126/science.aag0476>
- [28] Fan, P., Xie, Z., Liang, G., Ishaq, M., Chen, S., Zheng, Z., . . . , & Su, Z. (2021). High-efficiency ultra-thin Cu₂ZnSnS₄ solar cells by double-pressure sputtering with spark plasma sintered quaternary target. *Journal of Energy Chemistry*, 61, 186–194. <https://doi.org/10.1016/j.jechem.2021.01.026>

- [29] Gong, Y., Zhu, Q., Li, B., Wang, S., Duan, B., Lou, L., . . . , & Xin, H. (2022). Elemental de-mixing-induced epitaxial kesterite/CdS interface enabling 13%-efficiency kesterite solar cells. *Nature Energy*, 7(10), 966–977. <https://doi.org/10.1038/s41560-022-01132-4>
- [30] Green, M. A., Dunlop, E. D., Yoshita, M., Kopidakis, N., Bothe, K., Siefert, G., & Hao, X. (2023). Solar cell efficiency tables (version 62). *Progress in Photovoltaics: Research and Applications*, 31(7), 651–663. <https://doi.org/10.1002/pip.3726>
- [31] Cao, L., Wang, L., Zhou, Z., Zhou, T., Li, R., Zhang, H., . . . & Liu, S. (2024). Modifying surface termination by bidentate chelating strategy enables 13.77% efficient kesterite solar cells. *Advanced Materials*, 36(16), 2311918. <https://doi.org/10.1002/adma.202311918>
- [32] Baid, M., Hashmi, A., Jain, B., Singh, A. K., Susan, M. A. B. H., & Aleksandrova, M. (2021). A comprehensive review on $\text{Cu}_2\text{ZnSnS}_4$ (CZTS) thin film for solar cell: Forecast issues and future anticipation. *Optical and Quantum Electronics*, 53(11), 656. <https://doi.org/10.1007/s11082-021-03272-5>
- [33] Gupta, G. K., Chaurasiya, R., & Dixit, A. (2019). Theoretical studies on structural, electronic and optical properties of kesterite and stannite $\text{Cu}_2\text{ZnGe(S/Se)}_4$ solar cell absorbers. *Computational Condensed Matter*, 19, e00334. <https://doi.org/10.1016/j.cocom.2018.e00334>
- [34] Pu, A. (2018). *Modelling & simulations of $\text{Cu}_2\text{ZnSnS}_4$ thin film solar cell devices*. PhD Thesis, University of New South Wales. <https://doi.org/10.26190/unsworks/21220>
- [35] Sahu, M., Reddy, V. R. M., Park, C., & Sharma, P. (2021). Review article on the lattice defect and interface loss mechanisms in kesterite materials and their impact on solar cell performance. *Solar Energy*, 230, 13–58. <https://doi.org/10.1016/j.solener.2021.10.005>
- [36] Gao, Y., Yang, H., Zhang, Y., Li, J., Zhao, H., Feng, J., . . . , & Zheng, Z. (2014). Facile non-injection synthesis of high quality CZTS nanocrystals. *RSC Advances*, 4(34), 17667–17670. <https://doi.org/10.1039/c4ra01674b>
- [37] Annett, J. F. (1995). Efficiency of algorithms for Kohn-Sham density functional theory. *Computational Materials Science*, 4(1), 23–42. [https://doi.org/10.1016/0927-0256\(94\)00013-3](https://doi.org/10.1016/0927-0256(94)00013-3)
- [38] Banerjee, A. S., Elliott, R. S., & James, R. D. (2015). A spectral scheme for Kohn–Sham density functional theory of clusters. *Journal of Computational Physics*, 287, 226–253. <https://doi.org/10.1016/j.jcp.2015.02.009>
- [39] Davlatshoevich, N. D. (2021). Investigation optical properties of the orthorhombic system $\text{CsSnBr}_{3-x}\text{I}_x$: Application for solar cells and optoelectronic devices. *Journal of Human, Earth, and Future*, 2(4), 404–411. <https://doi.org/10.28991/hef-2021-02-04-08>
- [40] Dilshod, N., Kholmizro, K., Aliona, S., Fayzullaev, K., Viktoriya, G., & Tamerlan, K. (2023). On the optical properties of the $\text{Cu}_2\text{ZnSn}[\text{S}_{1-x}\text{Se}_x]_4$ system in the IR range. *Trends in Sciences*, 20(2), 4058. <https://doi.org/10.48048/tis.2023.4058>
- [41] Kananenka, A. A., Kohut, S. V., Gaiduk, A. P., Ryabinkin, I. G., & Staroverov, V. N. (2013). Efficient construction of exchange and correlation potentials by inverting the Kohn–Sham equations. *The Journal of Chemical Physics*, 139(7), 074112. <https://doi.org/10.1063/1.4817942>
- [42] Kato, T., & Saito, S. (2023). Kohn–Sham potentials by an inverse Kohn–Sham equation and accuracy assessment by virial theorem. *Journal of the Chinese Chemical Society*, 70(3), 554–569. <https://doi.org/10.1002/jccs.202200355>
- [43] Nematov, D. (2022). Influence of iodine doping on the structural and electronic properties of CsSnBr_3 . *International Journal of Applied Physics*, 7, 37–47.
- [44] Nematov, D. D., Kholmurodov, K. T., Yuldasheva, D. A., Rakhmonov, K. R., & Khojakhonov, I. T. (2022). Ab-initio study of structural and electronic properties of perovskite nanocrystals of the $\text{CsSn}[\text{Br}_{1-x}\text{I}_x]_3$ family. *HighTech and Innovation Journal*, 3(2), 140–150. <https://doi.org/10.28991/hij-2022-03-02-03>
- [45] Zhang, Y., Zhou, S., & Sun, K. (2023). $\text{Cu}_2\text{ZnSnS}_4$ (CZTS) for photoelectrochemical CO_2 reduction: Efficiency, selectivity, and stability. *Nanomaterials*, 13(20), 2762. <https://doi.org/10.3390/nano13202762>
- [46] Nematov, D. (2023). Bandgap tuning and analysis of the electronic structure of the Cu_2NiXS_4 (X= Sn, Ge, Si) system: mBJ accuracy with DFT expense. *Chemistry of Inorganic Materials*, 1, 100001. <https://doi.org/10.1016/j.cinorg.2023.100001>
- [47] Kresse, G., & Furthmüller, J. (1996). Efficiency of ab-initio total energy calculations for metals and semiconductors using a plane-wave basis set. *Computational Materials Science*, 6(1), 15–50. [https://doi.org/10.1016/0927-0256\(96\)00008-0](https://doi.org/10.1016/0927-0256(96)00008-0)
- [48] Perdew, J. P., Burke, K., & Ernzerhof, M. (1996). Generalized gradient approximation made simple. *Physical Review Letters*, 77(18), 3865–3868. <https://doi.org/10.1103/physrevlett.77.3865>
- [49] Sahní, V., Bohnen, K. P., & Harbola, M. K. (1988). Analysis of the local-density approximation of density-functional theory. *Physical Review A*, 37(6), 1895–1907. <https://doi.org/10.1103/physreva.37.1895>
- [50] Sun, J., Ruzsinszky, A., & Perdew, J. P. (2015). Strongly constrained and appropriately normed semilocal density functional. *Physical Review Letters*, 115(3), 036402. <https://doi.org/10.1103/physrevlett.115.036402>
- [51] Painter, G. S. (1981). Improved correlation corrections to the local-spin-density approximation. *Physical Review B*, 24(8), 4264–4270. <https://doi.org/10.1103/physrevb.24.4264>
- [52] Singh, D. J. (2010). Electronic structure calculations with the Tran-Blaha modified Becke-Johnson density functional. *Physical Review B*, 82(20), 205102. <https://doi.org/10.1103/physrevb.82.205102>
- [53] Beraich, M., Shaili, H., Benhsina, E., Hafidi, Z., Taibi, M., Bentiss, F., . . . , & Fahoime, M. (2020). Experimental and theoretical study of new kesterite $\text{Cu}_2\text{NiGeS}_4$ thin film synthesized via spray ultrasonic technic. *Applied Surface Science*, 527, 146800. <https://doi.org/10.1016/j.apsusc.2020.146800>
- [54] Chen, R., & Persson, C. (2017). Electronic and optical properties of Cu_2XSnS_4 (X = Be, Mg, Ca, Mn, Fe, and Ni) and the impact of native defect pairs. *Journal of Applied Physics*, 121(20), 203104. <https://doi.org/10.1063/1.4984115>
- [55] Deepika, R., & Meena, P. (2019). Preparation and characterization of quaternary semiconductor $\text{Cu}_2\text{NiSnS}_4$ (CNTS) nanoparticles for potential solar absorber materials. *Materials Research Express*, 6(8), 0850b7. <https://doi.org/10.1088/2053-1591/ab24e9>
- [56] Kamble, A., Mokurala, K., Gupta, A., Mallick, S., & Bhargava, P. (2014). Synthesis of $\text{Cu}_2\text{NiSnS}_4$ nanoparticles by hot injection method for photovoltaic applications. *Materials Letters*, 137, 440–443. <https://doi.org/10.1016/j.matlet.2014.09.065>
- [57] Qiu, X., Cao, B., Yuan, S., Chen, X., Qiu, Z., Jiang, Y., . . . , & Kanatzidis, M. G. (2017). From unstable CsSnI_3 to air-stable Cs_2SnI_6 : A lead-free perovskite solar cell light absorber with bandgap of 1.48 eV and high absorption coefficient. *Solar Energy Materials and Solar Cells*, 159, 227–234. <https://doi.org/10.1016/j.solmat.2016.09.022>
- [58] Jia, Z., Zhang, X., Gu, Z., & Wu, G. (2023). MOF-derived Ni-Co bimetal/porous carbon composites as electromagnetic

- wave absorber. *Advanced Composites and Hybrid Materials*, 6(1), 28. <https://doi.org/10.1007/s42114-022-00615-y>
- [59] Johnson, C. C., & Guy, A. W. (1972). Nonionizing electromagnetic wave effects in biological materials and systems. *Proceedings of the IEEE*, 60(6), 692–718. <https://doi.org/10.1109/proc.1972.8728>
- [60] Qian, S. B., Liu, G., Yan, M., & Wu, C. (2023). Lightweight, self-cleaning and refractory FeCo@MoS₂ PVA aerogels: From electromagnetic wave-assisted synthesis to flexible electromagnetic wave absorption. *Rare Metals*, 42(4), 1294–1305. <https://doi.org/10.1007/s12598-022-02191-y>
- [61] Zafar, M., Masood, M. K., Rizwan, M., Zia, A., Ahmad, S., Akram, A., . . . , & Shakil, M. (2019). Theoretical study of structural, electronic, optical and elastic properties of Al_xGa_{1-x}P. *Optik*, 182, 1176–1185. <https://doi.org/10.1016/j.ijleo.2018.12.165>
- [62] Kortüm, G. (2012). *Reflectance spectroscopy: Principles, methods, applications*. Germany: Springer. <https://doi.org/10.1007/978-3-642-88071-1>
- [63] Modest, M. F., & Mazumder, S. (2021). *Radiative heat transfer*. Netherlands: Elsevier.
- [64] Davlatshoevich, N. D., Islomovich, M. B., Temurjonovich, Y. M., & Tagoykulovich, K. K. (2023). Optimization optoelectronic properties Zn_xCd_{1-x}Te system for solar cell application: Theoretical and experimental study. *Biointerface Research in Applied Chemistry*, 13(1), 90. <https://doi.org/10.33263/briac131.090>
- [65] Khatun, M. M., Hosen, A., & Al Ahmed, S. R. (2023). Evaluating the performance of efficient Cu₂NiSnS₄ solar cell—A two stage theoretical attempt and comparison to experiments. *Heliyon*, 9(10), e20603. <https://doi.org/10.1016/j.heliyon.2023.e20603>
- [66] Khouja, O. E., Nouneh, K., Touhami, M. E., Matei, E., Stancu, V., Enculescu, M., & Galca, A. C. (2023). Growth and characterization of Cu–Ni–Sn–S films electrodeposited at different applied potentials. *Journal of Materials Science: Materials in Electronics*, 34(8), 760. <https://doi.org/10.1007/s10854-023-10173-8>
- [67] Kolhe, P., Musmade, B. B., Koinkar, P., Khedkar, S., Maiti, N., Kulkarni, S., & Sonawane, K. (2023). Study of physico-chemical properties of Cu₂NiSnS₄ thin films. *Modern Physics Letters B*, 37(16), 2340007. <https://doi.org/10.1142/S0217984923400079>
- [68] Mani, J., Radha, S., Rajkumar, R., Preethi, L., Veerappan, M., Arivanandhan, M., & Anbalagan, G. (2023). Tuning the structural, optical, thermal, and electrical properties of Cu₂NiSnS₄ through cobalt doping for thermoelectrical applications. *Journal of Solid State Chemistry*, 326, 124233. <https://doi.org/10.1016/j.jssc.2023.124233>
- [69] Nizomov, Z., Asozoda, M., & Nematov, D. (2023). Characteristics of nanoparticles in aqueous solutions of acetates and sulfates of single and doubly charged cations. *Arabian Journal for Science and Engineering*, 48(1), 867–873. <https://doi.org/10.1007/s13369-022-07128-2>
- [70] Schäfer, W., & Nitsche, R. (1974). Tetrahedral quaternary chalcogenides of the type Cu₂ II IV S₄ (Se₄). *Materials Research Bulletin*, 9(5), 645–654. [https://doi.org/10.1016/0025-5408\(74\)90135-4](https://doi.org/10.1016/0025-5408(74)90135-4)

How to Cite: Nematov, D. (2024). Analysis of the Optical Properties and Electronic Structure of Semiconductors of the Cu₂NiXS₄ (X = Si, Ge, Sn) Family as New Promising Materials for Optoelectronic Devices. *Journal of Optics and Photonics Research*, 1(2), 91–97. <https://doi.org/10.47852/bonviewJOPR42021819>